

Support Information

**Understanding Cascade Heterojunction of CuPc/Bi-MOF
for Photoelectrochemical Nitrate Reduction**

Yajie Bai,^{ab†} Zhenyuan Fang,^{c†} Meiqi Zhai,^b Xianlei Jiang,^a Jianming Li,^{*a} Hongye Bai,^{*b} Weiqiang Fan,^{*b}

^a *College of New Energy, Ningbo University of Technology, Ningbo, 315336, P. R. China.*

^b *School of Chemistry and Chemical Engineering, Jiangsu University, Zhenjiang, 212013, P. R. China.*

^c *School of Chemistry, Beihang University, Beijing, 100191, P. R. China*

[†] *These authors contributed equally to this work.*

**Emails: fwq4993329@ujs.edu.cn (W. Fan), bhy198412@163.com (H. Bai),
jmli@nbut.edu.cn (J. Li).*

Materials

All chemical reagents are of analytical grade and are used without further purification. Copper phthalocyanine (CuPc), Bismuth nitrate pentahydrate ($\text{Bi}(\text{NO}_3)_3 \cdot 5\text{H}_2\text{O}$), 1,3,5-Benzenetricarboxylic acid (H_3BTC), Potassium nitrate (KNO_3), Ammonium chloride (NH_4Cl), Sodium nitrite (NaNO_2), sodium sulfite (Na_2SO_3), nitric acid and sodium potassium tartrate ($\text{NaKC}_4\text{H}_4\text{O}_6$), Nessler's reagent, hydrogen nitrate (HNO_3 , 65%~68%) were all obtained from Aladdin Reagent Co. The FTO glass substrates used in the experiment were washed by acetone and ethanol for 25 minutes in advance.

Characterization

The morphology of samples was investigated by transmission electron microscopy (TEM, Tecnai G2 F20 S-Twin electron microscope (FEI Co.)), and scanning electron microscopy (SEM, Hitachi S-4800 25.0kV 7.5mm×40.0 SE(U)). The crystal structure was collected by high-resolution transmission electron microscope (HRTEM) and X-ray diffractometer (XRD, Bruker D8 ADVANCE). The valence state and composition of elements were detected by X-ray photoelectron spectroscopy (XPS, Thermo Fisher Scientific, Escalab 250Xi, Al Ka). Fourier-transform infrared spectroscopy (FT-IR) to systematically evaluate the structure and morphology of the CuPc/Bi-MOF material. Electrochemical impedance spectroscopy (EIS) and Mott-Schottky data were tested by electrochemical instrumentation (Princeton, VersaSTAT 3). The absorption spectra were tested by UV-Vis 2550 (Shimadzu, Japan). All photoelectrochemical tests were carried out on the

electrochemical system (CHI-614, China).

Preparation

CuPc was prepared by vacuum evaporation method as follows: The cleaned FTO was fixed to the top of the vacuum evaporation system, and 0.2 g of CuPc powder was added to the metal evaporation crucible. Open the vacuum pump, reduce the vacuum degree of the system to 10^{-3} Pa, and start the heating system to keep the FTO rotating evenly. After heating for 5 min, a uniform film of blue CuPc was successfully formed on the FTO surface.

CuPc/Bi-MOF was prepared by chemical bath deposition using CuPc as the substrate material, detailed as follows: First, the prepared CuPc samples were soaked with solutions containing 20 mmol $\text{Bi}(\text{NO}_3)_3 \cdot 5\text{H}_2\text{O}$ for 5, 10, 15, 20, 25 min to deposit Bi-MOF layers of different thicknesses. Subsequently, the samples were transferred to an ethanol solution to remove excess water. Next, the sample was again dipped into a solution containing 20 mmol H3BTC for the same time. This step ensures that the Bi-MOF layer is successfully deposited on the CuPc surface. Finally, the CuPc/Bi-MOF was obtained as the final MOF cathode.

PEC Measurements

All photoelectrochemical testing was conducted in a 0.1 M phosphate buffer solution (PBS) using a three-electrode system with CuPc/Bi-MOF as the working electrode, Ag/AgCl as the reference electrode, and a Pt foil as the counter electrode, under simulated sunlight illumination provided by a 100 mW cm^{-2} xenon lamp in a sealed H-cell (Scheme S2). Measurements were taken using linear sweep

voltammetry and cyclic voltammetry techniques in PBS containing $150 \mu\text{g mL}^{-1}$ KNO_3 and $150 \mu\text{g mL}^{-1}$ KCl , with Mott-Schottky plots generated at 500 and 800 Hz frequencies for both CuPc and CuPc/Bi-MOF.

The determination of $\text{NH}_3\text{-N}$

First, the NH_4Cl crystals were dried overnight at $105\text{-}110^\circ\text{C}$ to prepare 50 mL NH_4Cl solutions at different concentrations (0.0, 0.2, 0.4, 0.6, 0.8, $1.0 \mu\text{g mL}^{-1}$). Next, add 1 mL $\text{NaKC}_4\text{H}_4\text{O}_6$ (500 g L^{-1}) and 1 mL of Nessler's reagent to each solution and leave to stand for about 20 min. Absorbance was measured at 425 nm by a UV-vis spectrophotometer to establish a relationship between absorbance and $\text{NH}_3\text{-N}$ concentration. The results showed a good linear relationship between the absorbance and the $\text{NH}_3\text{-N}$ concentration ($y = 0.1751x + 0.00564$, $R^2 = 0.9999$) (Fig. S12 and S13). The concentration of $\text{NH}_3\text{-N}$ in the reaction solution was determined by the same method to calculate the NH_3 yield:

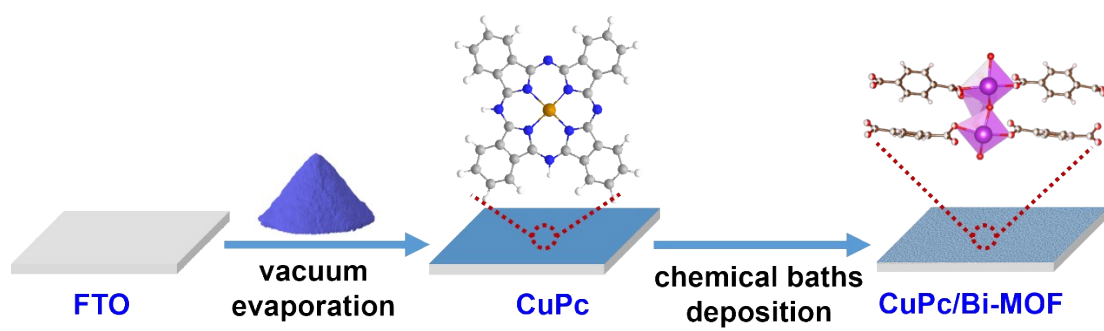
$$V_{\text{NH}_3} = (C_{\text{NH}_3} \times V) / (T \times S)$$

Among them, C_{NH_3} represents the measured NH_3 concentration, V is the reaction liquid product, S is the cathode area, and T is the reaction time.

Determination of $\text{NO}_2\text{-N}$

For the determination of $\text{NO}_2\text{-N}$ concentration, a Griess chromoagent was first prepared: 0.2 g of N-(1-naphthyl) diethyldiamine hydrochloride, 4 g of p-aminophenylsulfonamide and 10 mL of phosphoric acid ($\rho = 1.70 \text{ g mL}^{-1}$) were mixed in 50 mL of deionized water. 0.1 mL of chromogen was mixed with 5 mL of $\text{NO}_2\text{-N}$ solution (0.00, 0.02, 0.04, 0.06, 0.10, $0.20 \mu\text{g mL}^{-1}$; NaNO_2 crystals were

dried at 105-110 °C for 2 h before use) and left for 20 min, the absorbance was measured at 540 nm. Show a good linear relationship between the obtained absorbance and the NO₂⁻-N concentration ($y = 0.7850x - 0.0058$, $R^2 = 0.9998$) (Fig. S14 and S15). The amount of NO₂⁻-N in the reaction solution was determined by the same method.



Scheme S1 Schematic illustration of the synthesis process of CuPc/Bi-MOF.

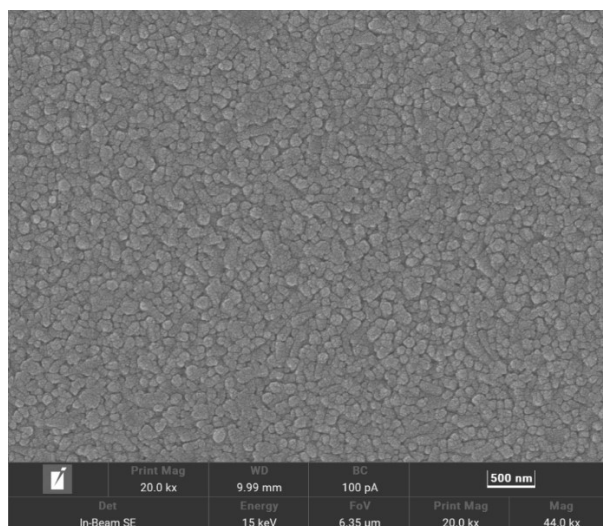


Fig. S1 SEM image of CuPc.

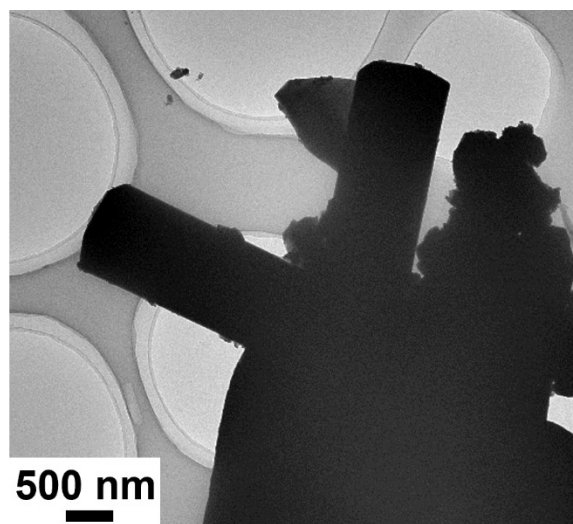


Fig. S2 TEM image of CuPc/Bi-MOF.

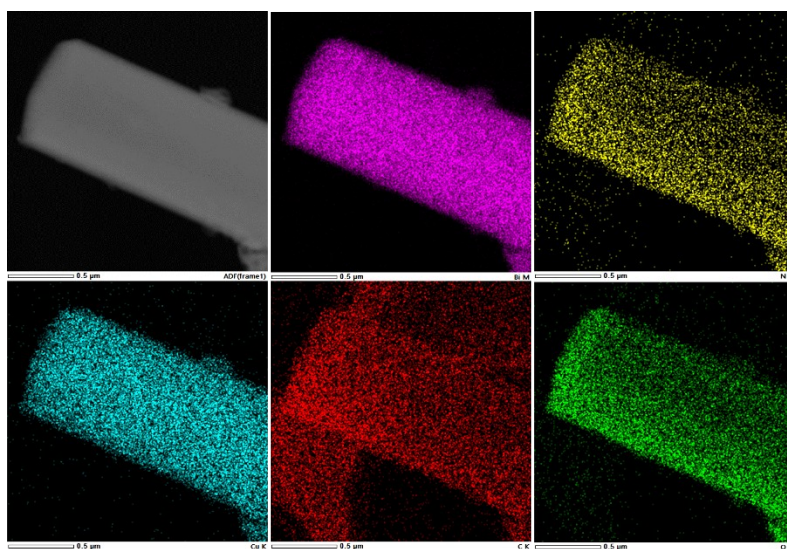


Fig. S3 Elemental mapping images of CuPc/Bi-MOF.

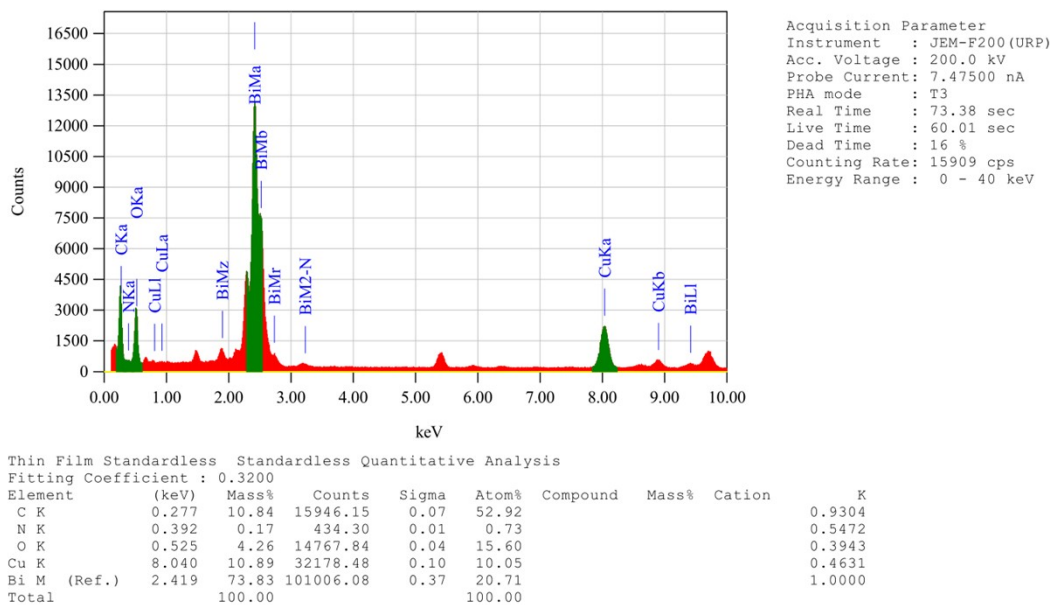


Fig. S4 Quantitative analysis images of CuPc/Bi-MOF.

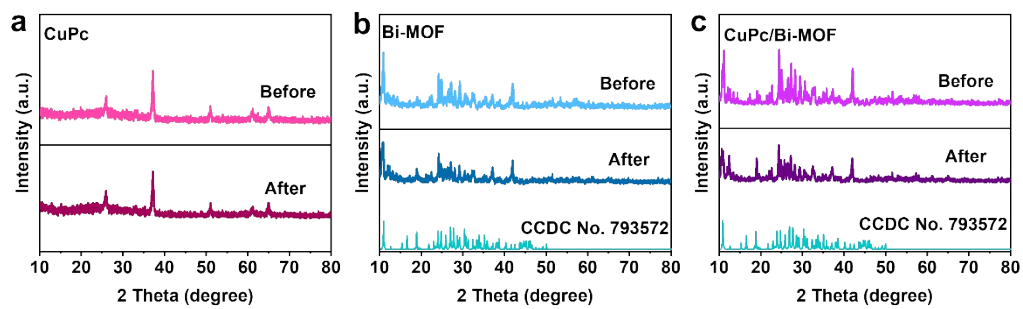


Fig. S5 XRD patterns before and after measurements.

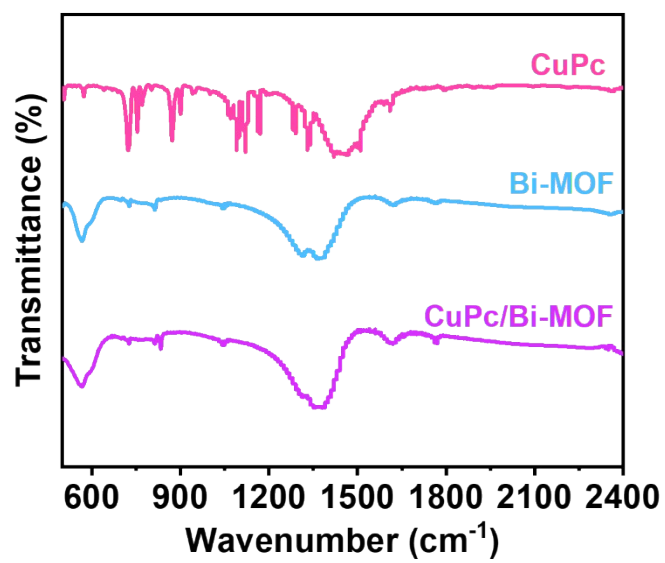


Fig. S6 FTIR images of CuPc, Bi-MOF and CuPc/Bi-MOF.

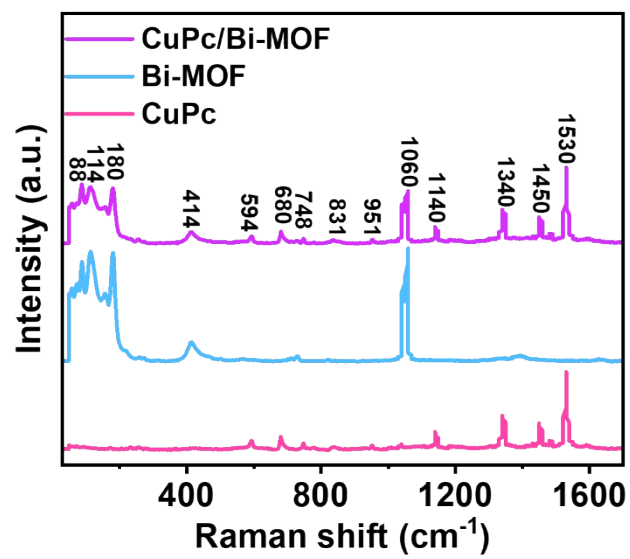


Fig. S7 Raman images of CuPc, Bi-MOF and CuPc/Bi-MOF.

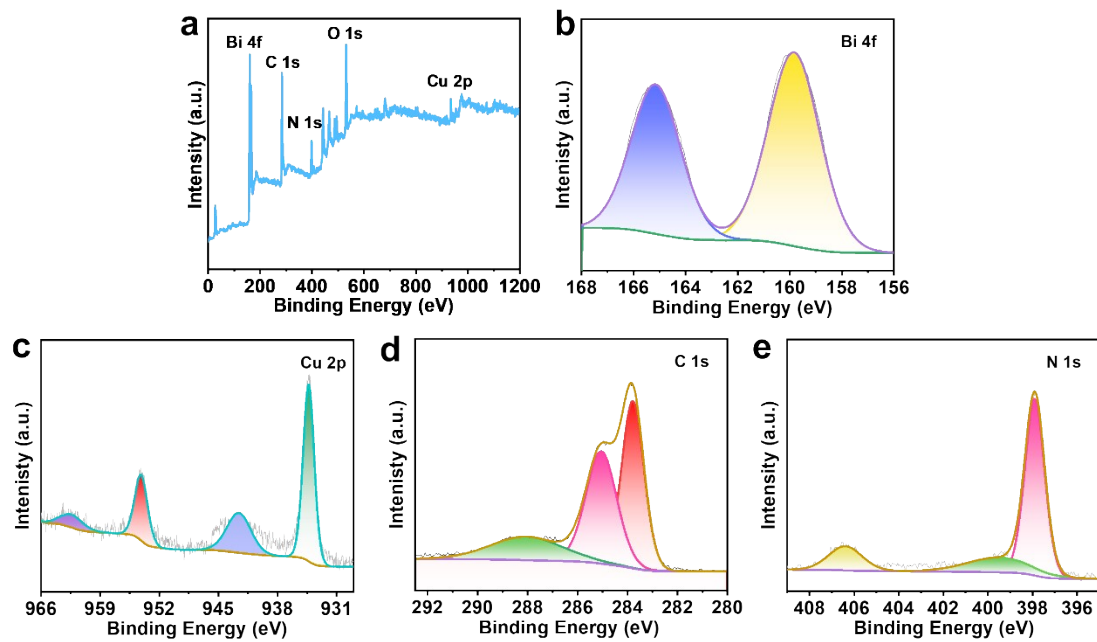


Fig. S8 High-resolution XPS spectra of CuPc/Bi-MOF: (a) full spectrum, (b) Bi 4f, (c) Cu 2p, (d) C 1s, (e) N 1s.

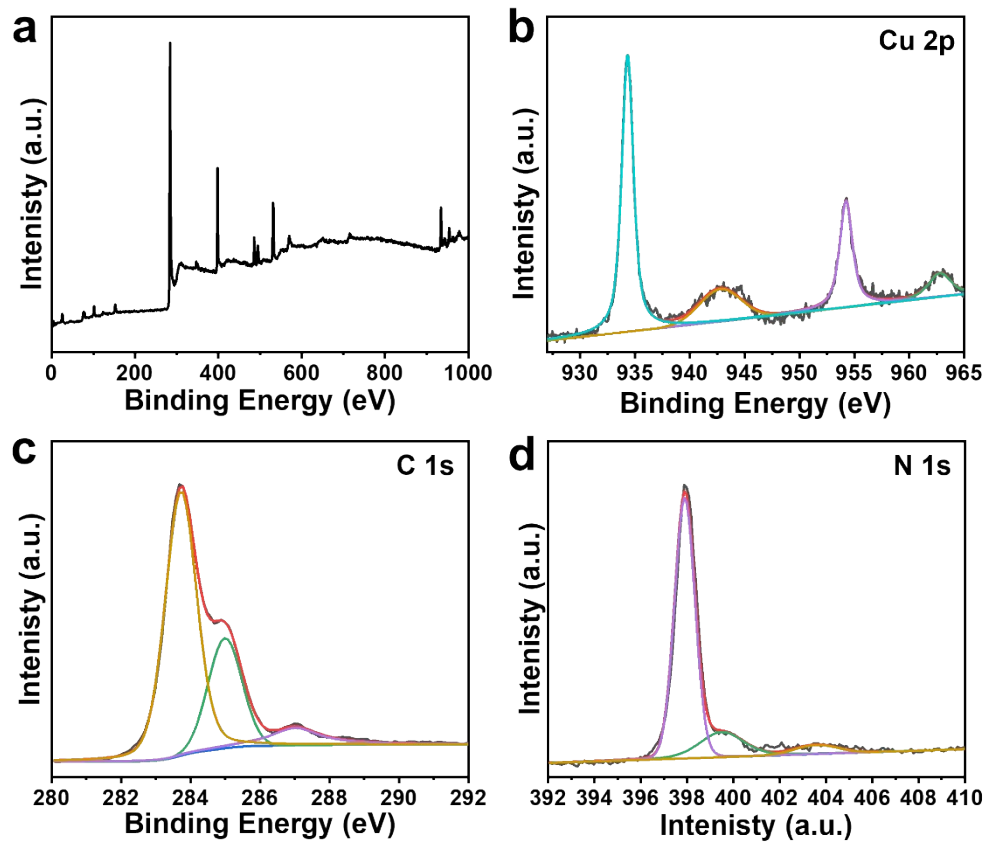


Fig. S9 High-resolution XPS spectra of CuPc: (a) full spectrum, (b) Cu2p XPS spectra, (c) C1s XPS spectra, (d) N1s XPS spectra.

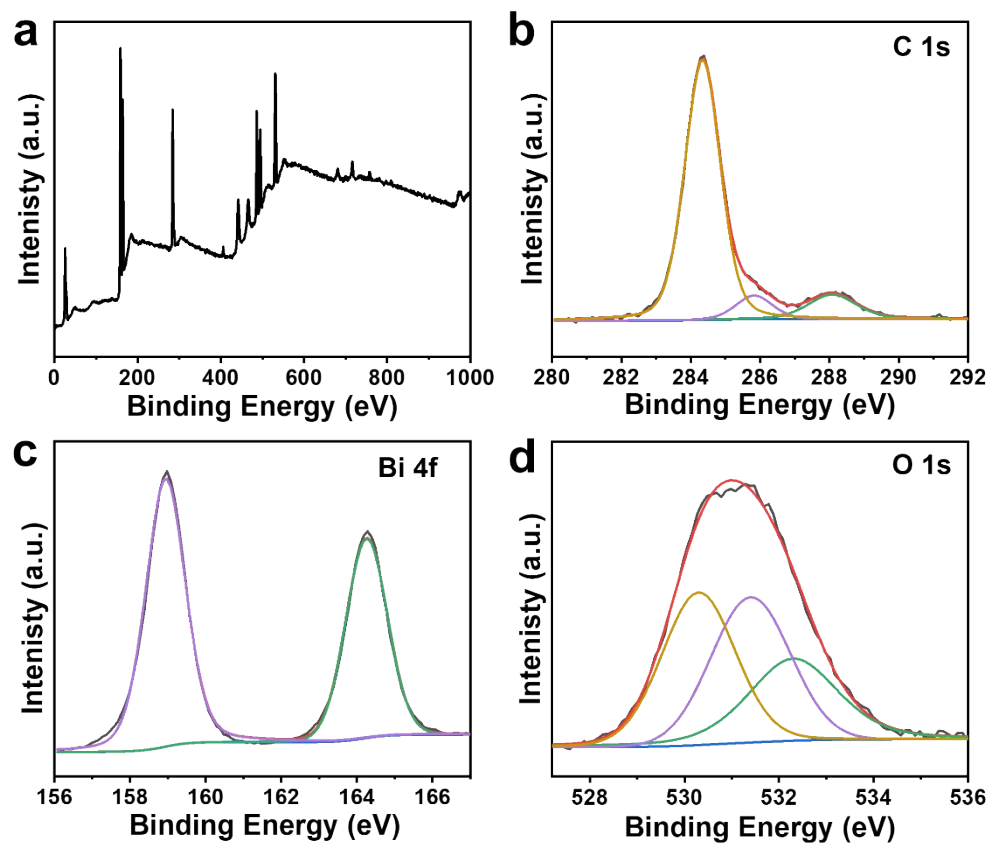


Fig. S10 High-resolution XPS spectra of Bi-MOF: (a) full spectrum, (b) C 1s XPS spectra, (c) Bi 4f XPS spectra, (d) O 1s XPS spectra.

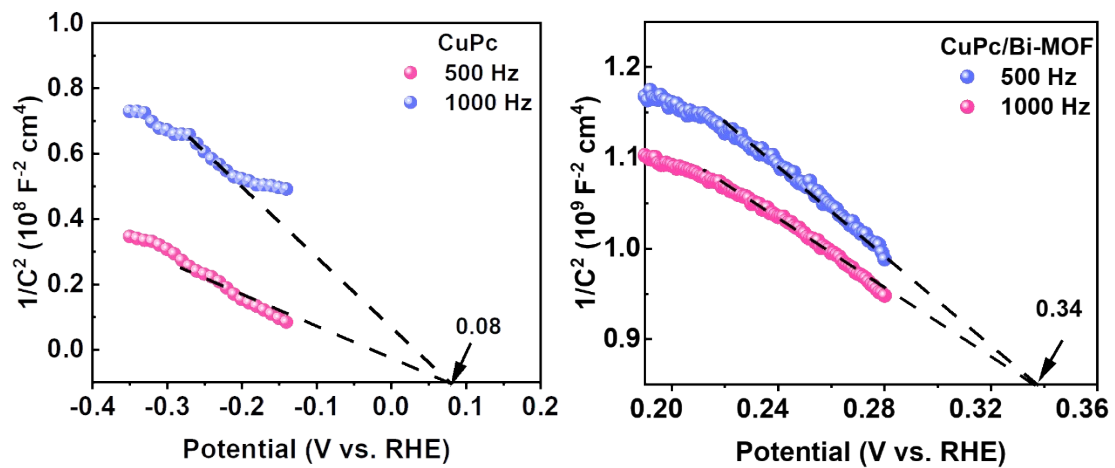
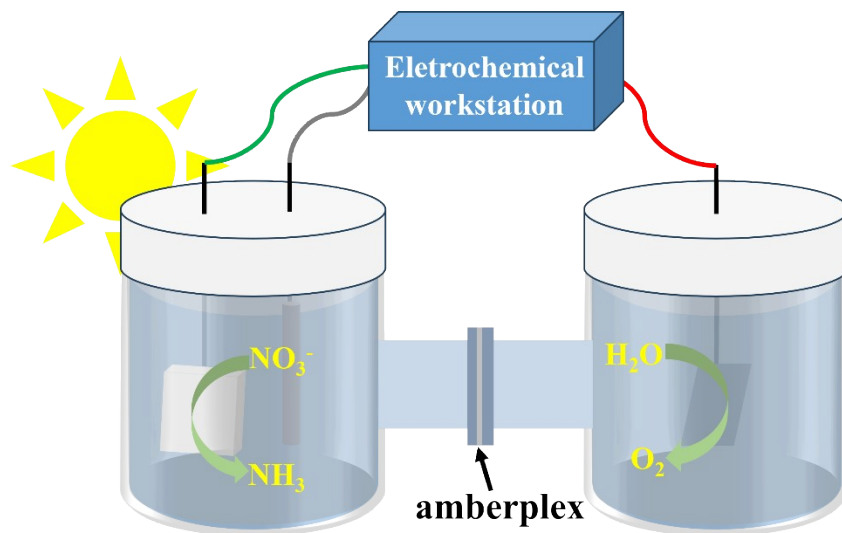


Fig. S11 Mott-Schottky plots of CuPc and CuPc/Bi-MOF.



Scheme S2 The schematic diagram for PEC NITRR configuration.

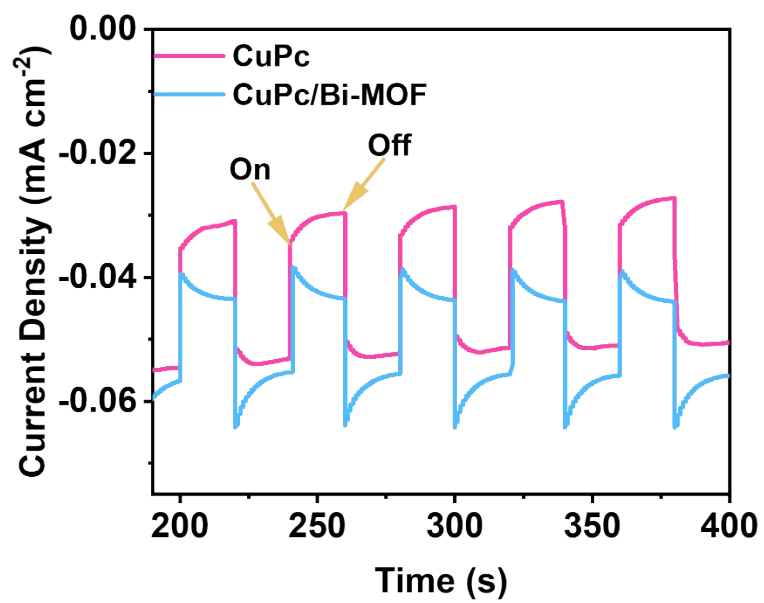


Fig. S12 I-t curves under cyclic switching illumination of CuPc and CuPc/Bi-MOF.

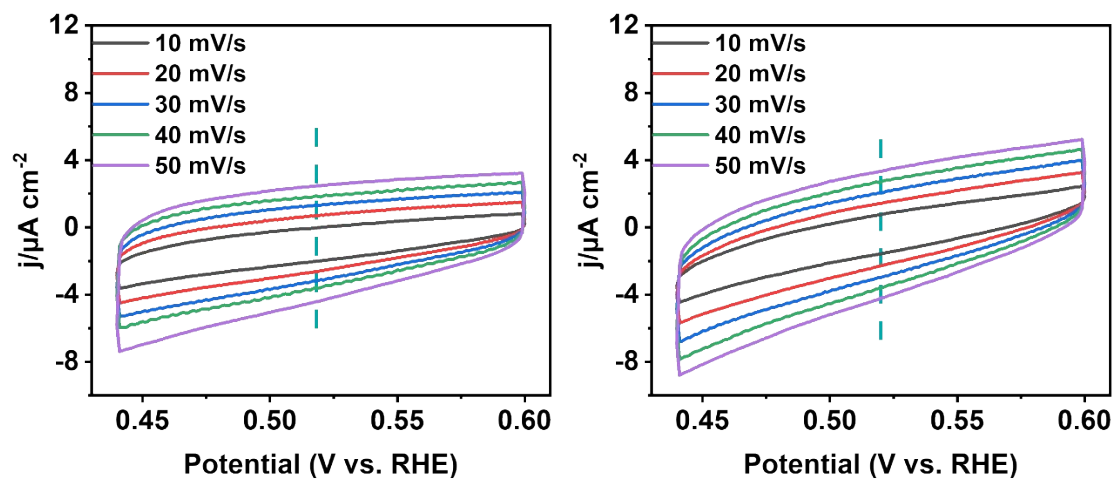


Fig. S13 Cyclic voltammetry measurements with different scanning rates of CuPc and CuPc/Bi-MOF.

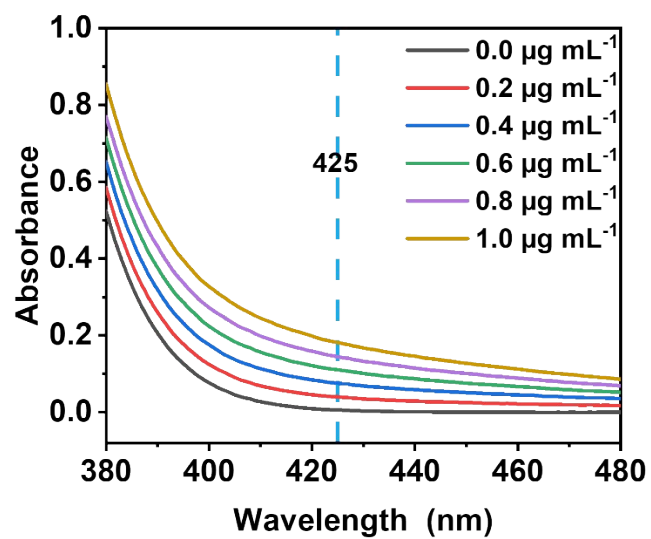


Figure S14. Standard absorbance curve of NH₃ yield by Nessler reagent spectrophotometry.

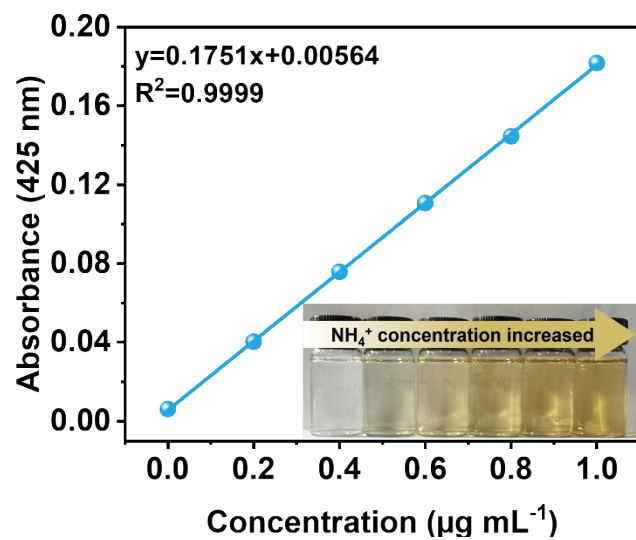


Figure S15. Calibration curve of NH_3 yield by Nessler reagent spectrophotometry.

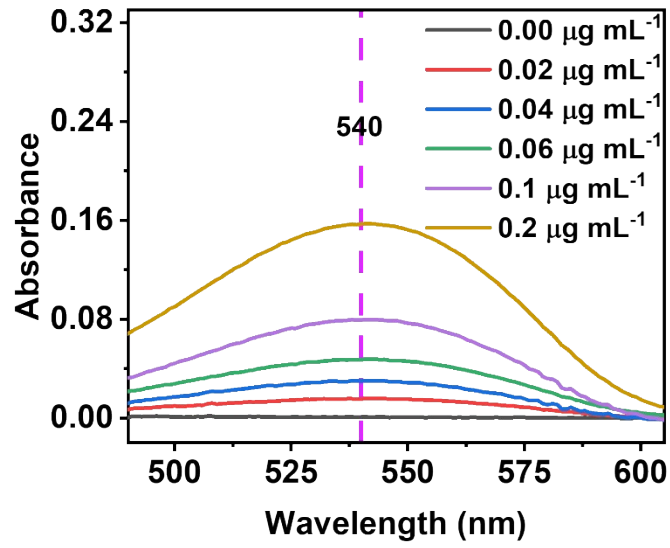


Figure S16. Standard absorbance curve of NO_2^- yield by Griess reagent spectrophotometry method.

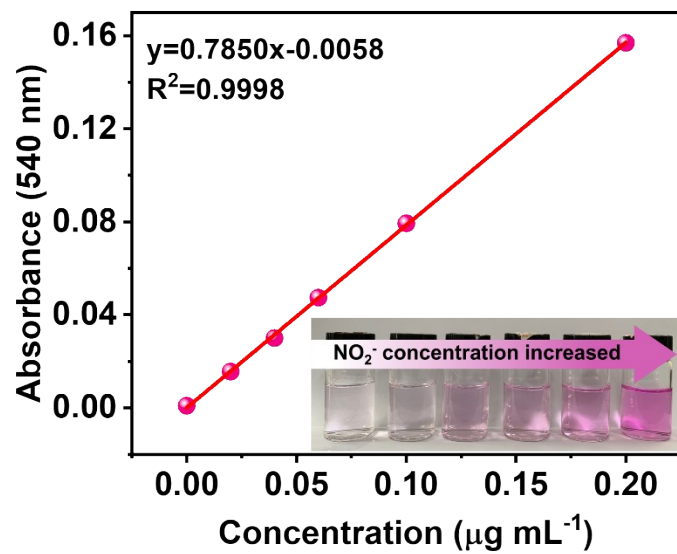


Figure S17. Standard absorbance curve of NH_3 yield by Nessler reagent spectrophotometry.

Catalyst	Yield ($\mu\text{g h}^{-1} \text{cm}^{-2}$)	Ref.
Pt	0.191	[S1]
$\text{Fe}_3\text{O}_4/\text{Ti}$	2.0	[S2]
Ag nanosheet	2.8	[S3]
Bi-doped CeO_2	6.3	[S4]
MoO	6.8	[S5]
NiO/CuPc	7.13	This work

Table S1. All data about NH_3 yield rate have been unified as “ $\mu\text{g h}^{-1} \text{cm}^{-2}$ ” for comparison.

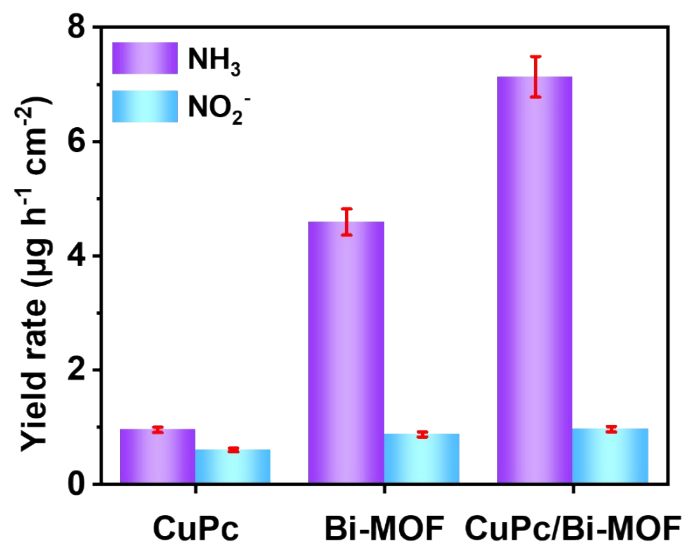


Fig. S18 NH_3 and NO_2^- yield rate of CuPc, Bi-MOF and CuPc/Bi-MOF at 0 V vs. RHE.

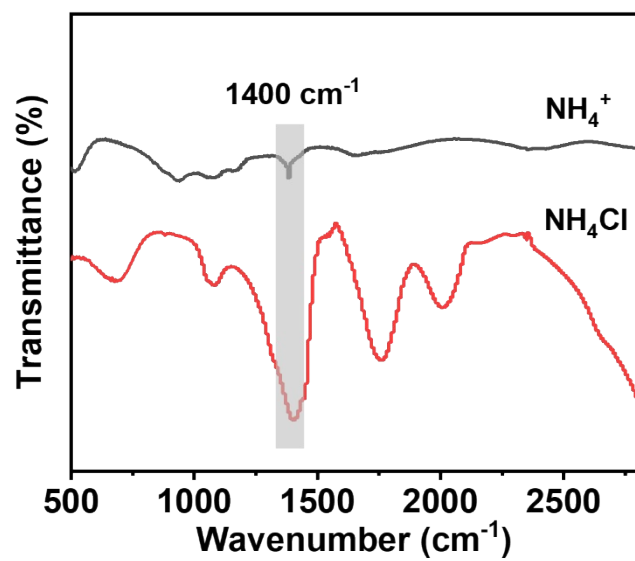


Fig. S19 FTIR test after 12 h of reaction.

- [S1] B. Sheets, G. Bott, *ChemComm*. 2018, **54**, 4250–4253.
- [S2] Q. Liu, X. Zhang, B. Zhang, Y. Luo, G. Cui, F. Xie, A. Asiri, X. Sun, *Nanoscale*, 2018, **10**, 14396–14389.
- [S3] H. Huang, X. Li, X. Shi, A. Asiri, *Chem. Commun.* 2018, **54**, 11427–11430.
- [S4] Y. Liu, C. Li, L. Guan, K. Li, Y. Lin, *J. Phys. Chem. C* 2020, **124**, 18003–18009.
- [S5] X. Qu, L. Shen, Y. Mao, J. Lin, Y. Li, G. Li, Y. Zhang. G. Li, Y. Zhang, Y. Jiang, S. Sun, *ACS Appl. Mater. Interfaces* 2019, **11**, 31869–31877.